An Experimental and Theoretical Study of the Long-Lived Radical Cation of $CH_3OCH_2CH_2OH$

Jaana M. H. Pakarinen,[†] Rebecca L. Smith,[‡] Pirjo Vainiotalo,*[,†] Tapani A. Pakkanen,*[,†] and Hilkka I. Kenttämaa*[,‡]

Contribution from the Departments of Chemistry, University of Joensuu, FIN-80101 Joensuu, Finland, and Purdue University, West Lafayette, Indiana 47907-1393

Received June 29, 1995[⊗]

Abstract: The long-lived radical cation of 2-methoxyethanol, $CH_3OCH_2CH_2OH^{\bullet+}$, is stable toward isomerization in the gas phase. This radical cation reacts with neutral reagents via three main channels in a Fourier-transform ion cyclotron resonance mass spectrometer. $CH_3OCH_2CH_2OH^{\bullet+}$ abstracts an electron from reagents with ionization energies less than that of $CH_3OCH_2CH_2OH$. Neutral reagents with higher ionization energies replace $CH_3OCH_2^{\bullet}$ or CH_2O in the ion. Both replacement reactions are probably driven by the formation of a hydrogen bond between the entering nucleophile and the hydroxyl group in $CH_3OCH_2CH_2OH^{\bullet+}$, which breaks the C−C bond in CH_3OCH_2-$CH_2OH^{\bullet+}$. For strong nucleophiles, this process is so exothermic that the resulting ion/molecule complex dissociates by loss of $CH_3OCH_2^{\bullet}$. However, weak nucleophiles yield a longer-lived ion−molecule complex. Within this complex, $CH_3OCH_2^{\bullet}$ can react with the initially produced ion by replacement of CH_2O (a weaker nucleophile) to yield the hydrogen-bridged complex of $CH_3OCH_2^{\bullet}$ and the nucleophile. *This reaction provides a general approach for the gas-phase synthesis of different hydrogen-bridged radical cations. Ab initio* molecular orbital calculations suggest that the most stable geometry of $CH_3OCH_2CH_2OH^{\bullet+}$ is characterized by an unusually long C−C bond (1.775 Å at the UMP2/6-31G** level of theory). This finding is in agreement with the observed facile cleavage of the C−C bond in $CH_3OCH_2CH_2OH^{\bullet+}$. The isomeric ions $^{\bullet}CH_2O^+(CH_3)CH_2OH$, $(CH_3)_2O^+CH_2O^{\bullet}$, $^{\bullet}CH_2OCH_2CH_2OH_2^+$, $^{\bullet}CH_2O(CH_3)-H^+\cdots O{=}CH_2$, and $CH_3OC(H)H\cdots O(H){=}CH_2^{\bullet+}$ were calculated to be less stable than $CH_3OCH_2CH_2$-$OH^{\bullet+}$ (at the UMP2/6-31G**//UHF/6-31G**+ZPE level of theory). Only the ion $(CH_3)_2O$-$H\cdots O{=}CH^{\bullet+}$ was found to lie lower in energy than $CH_3OCH_2CH_2OH^{\bullet+}$ (by 7.2 kcal/mol at the UMP2/6-31G**+ZPVE level of theory). However, experimental evidence does not support the formation of this hydrogen-bridged ion upon ionization of 2-methoxyethanol.

Introduction

The removal of an electron from an organic molecule often significantly affects its structure, relative thermodynamic stability, and the barrier heights for isomerization and dissociation.[1] Isomerization reactions are common for organic radical cations. Indeed, the combined results obtained from mass spectrometry experiments and high-level *ab initio* molecular orbital calculations have demonstrated that radical cations formed upon removal of an electron from a stable neutral molecule can be significantly less stable than their nonconventional isomers with no stable neutral counterparts. Such nonconventional radical cations include hydrogen-bridged radical cations and distonic radical cations (*i.e.*, ionized ylides, zwitterions, or biradicals).[1−16] Both types of ions have been established to represent stable gas-phase species.[1,4,6b,13]

The 2-methoxyethanol radical cation $CH_3OCH_2CH_2OH^{\bullet+}$ (**1**) undergoes interesting unimolecular dissociation reactions,[16−22] some of which have been proposed to involve hydrogen-bridged

† University of Joensuu.
‡ Purdue University.
⊗ Abstract published in *Advance ACS Abstracts,* April 15, 1996.

(1) Roth, H. D. In *Topics in Current Chemistry*; Springer-Verlag: Berlin, 1992; Vol. 163.
(2) (a) McAdoo, D. J. *Mass Spectrom. Rev.* **1988**, *7*, 363. (b) Longevialle, P. *Mass Spectrom. Rev.* **1992**, *11*, 157.
(3) Heinrich, N.; Schwarz, H. *Ion and Cluster Ion Spectroscopy and Structure*; Maier, J. P., Ed.; Elsevier: Amsterdam, 1989; pp 329−372.
(4) (a) Pakarinen, J. M. H.; Vainiotalo, P.; Pakkanen, T. A.; Kenttämaa, H. I. *J. Am. Chem. Soc.* **1993**, *115*, 12431. (b) George, M.; Kingsmill, A. C.; Suh, D.; Terlouw, J. K.; Holmes, J. L. *J. Am. Chem. Soc.* **1994**, *116*, 7807.
(5) Postma, R.; Ruttink, P. J. A.; van Duijneveldt, F. B.; Terlouw, J. K.; Holmes, J. L. *Can. J. Chem.* **1985**, *63*, 2798.
(6) (a) Burgers, P. C.; Holmes, J. L.; Hop, C. E. C. A.; Postma, R.; Ruttink, P. J. A.; Terlouw, J. K. *J. Am. Chem. Soc.* **1987**, *109*, 7315. (b) Hoke, S. H., II; Yang, S. S.; Cooks, R. G.; Hrovat, D. A.; Borden, W. T. *J. Am. Chem. Soc.* **1994**, *116*, 4888.
(7) van Baar, B. L. M.; Burgers, P. C.; Holmes, J. L.; Terlouw, J. K. *Org. Mass Spectrom.* **1988**, *23*, 355.
(8) Postma, R.; van Helden, S. P.; van Lenthe, J. H.; Ruttink, P. J. A.; Terlouw, J. K.; Holmes, J. L. *Org. Mass Spectrom.* **1988**, *24*, 503.
(9) van Driel, J. H.; Heerma, W.; Terlouw, J. K.; Halim, H.; Schwarz, H. *Org. Mass Spectrom.* **1985**, *20*, 665.
(10) Cao, J. R.; George, M.; Holmes, J. L.; Sirois, M.; Terlouw, J. K.; Burgers, P. C. *J. Am. Chem. Soc.* **1992**, *114*, 2017.
(11) Heinrich, N.; Schmidt, J.; Schwarz, H.; Apeloig, Y. *J. Am. Chem. Soc.* **1987**, *109*, 1317.
(12) (a) Postma, R.; Ruttink, P. J. A.; van Baar, B.; Terlouw, J. K.; Holmes, J. L.; Burgers, P. C. *Chem. Phys. Lett.* **1986**, *123*, 409. (b) Burgers, P. C.; Lifshitz, C.; Ruttink, P. J. A.; Schaftenaar, G.; Terlouw, J. K. *Org. Mass Spectrom.* **1989**, *24*, 579.
(13) For recent reviews, see: (a) Hammerum, S. *Mass Spectrom. Rev.* **1988**, *7*, 123. (b) Stirk, K. M.; Kiminkinen, M.; Kenttämaa, H. I. *Chem. Rev.* **1992**, *92*, 1649.
(14) Schaftenaar, G.; Postma, R.; Ruttink, P. J. A.; Burgers, P. C.; McGibbon, G. A.; Terlouw, J. K. *Int. J. Mass Spectrom. Ion Processes* **1990**, *100*, 521.
(15) McGibbon, G. A.; Kingsmill, C. A.; Terlouw, J. K.; Burgers, P. C. *Org. Mass Spectrom.* **1992**, *27*, 126.
(16) See, for example: Wesdemiotis, C.; Polce, M. J. *J. Am. Soc. Mass Spectrom.* **1995**, *6*, 1030 and references therein.
(17) (a) Morton, T. H. *Tetrahedron* **1982**, *38*, 3195. (b) Biermann, H. W.; Morton, T. H. *J. Am. Chem. Soc.* **1983**, *105*, 5025.
(18) Vazquez, S.; Mosquera, R. A.; Rios, M. A.; van Alsenoy, C. *J. Mol. Struct. (Theochem)* **1989**, *188*, 95.
(19) Ruttink, P. J. A.; Burgers, P. C. *Org. Mass Spectrom.* **1993**, *28*, 1087.
(20) Audier, H. E.; Milliet, A.; Leblanc, D.; Morton, T. H. *J. Am. Chem. Soc.* **1992**, *114*, 2020.
(21) Cao, J. R.; George, J. L.; Holmes, J. L.; Sirois, M.; Terlouw, J. K.; Burgers, P. C. *J. Am. Chem. Soc.* **1992**, *114*, 2017.

0002-7863/96/1518-3914$12.00/0

Scheme 1

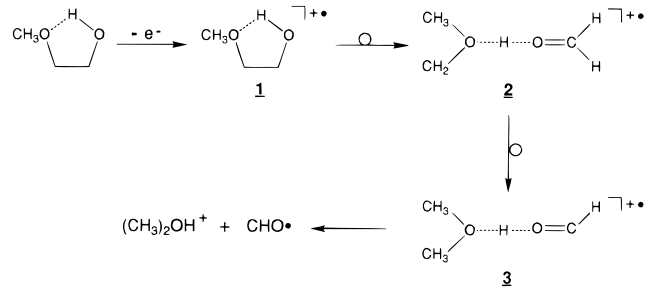

and/or distonic radical cation intermediates. The strong intramolecular hydrogen bond[18] in the neutral $CH_3OCH_2CH_2OH$ was initially thought to remain after ionization (**1**, Scheme 1) and to lead to isomerization of the initially formed radical cation to a hydrogen-bridged complex of formaldehyde and the methoxymethyl radical, $CH_3O(CH_2)\cdots H\cdots O{=}CH_2^{\bullet+}$ (**2**, Scheme 1).[17] This ion was suggested to undergo a hydrogen atom shift to yield another hydrogen-bridged intermediate, $(CH_3)_2O\cdots H\cdots O{=}CH^{\bullet+}$ (**3**), which decomposes by expulsion of CHO$^{\bullet}$. A similar mechanism was proposed[19] for the loss of CHO$^{\bullet}$ from the molecular ion of ethylene glycol, but this mechanism was later proved to be incorrect through labeling experiments.[20,21]

The role of hydrogen-bridged intermediates in the dissociation of $CH_3OCH_2CH_2OH^{\bullet+}$ was reinvestigated[20,21] by using differently deuterated analogues of $CH_3OCH_2CH_2OH$. The results convincingly demonstrate that the mechanism initially proposed for the CHO$^{\bullet}$ loss must be incorrect. Various findings, including the observation of extensive intramolecular hydrogen scrambling involving all the hydrogen atoms except the methylene hydrogens in CH_2OH, were rationalized by the intermediacy of the distonic ions $^{\bullet}CH_2O^+(CH_3)CH_2OH$ (**4**) and $(CH_3)_2O^+CH_2O^{\bullet}$ (**5**) in the pathway leading to loss of CHO$^{\bullet}$ (Scheme 2). The mechanism proposed[20] for this dissociation involves the cleavage of the C−C bond, rotation of a methylene group, and C−O bond formation to generate the distonic ion $^{\bullet}CH_2O^+(CH_3)CH_2OH$ (**4**). Migration of the hydroxylic hydrogen to the terminal methylene carbon yields the other distonic ion, $(CH_3)_2O^+CH_2O^{\bullet}$ (**5**), which dissociates to yield protonated dimethyl ether and CHO$^{\bullet}$. Another dissociation pathway, loss of water, was proposed to occur via formation of a third distonic ion, $^{\bullet}CH_2OCH_2CH_2OH_2^+$ (**6**, Scheme 2).[20] Recent results[16] suggest that this reaction yields $^{\bullet}CH_2CH_2OCH_2^+$ and a minor amount of $CH_2{=}CHOCH_3^{\bullet+}$ and not the oxetane radical cation proposed[20] earlier.

The above investigations convincingly ruled out hydrogen-bridged complexes as reactive intermediates during dissociation of $CH_3OCH_2CH_2OH^{\bullet+}$, while providing support for the equilibration of three different distonic ions with the internally excited radical cation $CH_3OCH_2CH_2OH^{\bullet+}$. These intriguing findings raise a question concerning the structure of the *nonfragmenting, long-lived* $CH_3OCH_2CH_2OH^{\bullet+}$. The present study shows that the long-lived radical cation generated upon ionization of $CH_3OCH_2CH_2OH$ is stable toward isomerization. *Ab initio* molecular orbital calculations carried out at the UMP2/6-31G** level of theory suggest that the most stable conformer of $CH_3OCH_2CH_2OH^{\bullet+}$ is characterized by an unusually long C−C bond. This bond is readily cleaved upon gas-phase reactions with neutral reagents.

Experimental and Theoretical Methods

All experiments were carried out using an Extrel Fourier-transform ion cyclotron resonance mass spectrometer (Model 2001 FT/MS system) equipped with 3 T superconducting magnet (operated at 2.3 T), described in detail previously.[4a] The cell was differentially pumped with two turbomolecular pumps (Balzers TPU 330) to achieve a base pressure of $<1 \times 10^{-9}$ Torr in each cell, as read by an ionization gauge. Reagents were introduced by using either a pulsed valve inlet system or one of two Extrel FT/MS heated batch inlet systems equipped with variable leak valves.

"Chirp" excitation (2.7 MHz bandwidth, 124 V_{p-p} amplitude, 3.0−3.1 kHz/μs sweep rate) was used to excite ions for detection. The spectra were subjected to one zero fill prior to Fourier transformation, and they were recorded as 32K data points at a digitizer rate of 5.3 MHz. The spectra shown are an average of ≥15 acquisitions.

The radical cation of $CH_3OCH_2CH_2OH^{\bullet+}$ was generated from methoxyethanol introduced into one side of the dual cell by electron ionization or by electron abstraction using $CS_2^{\bullet+}$ reagent ions (ionization energies[23a] (IE) of CS_2 and $CH_3OCH_2CH_2OH$ are 10.07 and 9.6 eV, respectively). The electron energy (20−75 eV), emission current (2−10 μA), and ionization time (5−50 ms) were optimized separately for each experiment. Undesired ions generated by the electron beam in the other side of the dual cell were removed by applying a negative potential on the remote trapping plate of this cell. The ions remaining in the other cell were then transferred into the cleaned cell by grounding the conductance limit plate for 100 μs and collisionally cooled with argon pulsed into the cell. The radical cation of $CH_3OCH_2CH_2OH$ (*m*/*z* 76) was isolated through the use of the Stored Waveform Inverse Fourier Transform (SWIFT)[24] excitation method (Extrel FTMS SWIFT Module). The molecular ion was then allowed to react with a selected neutral reagent for a variable time period. Primary products were identified based on their constant branching ratios at short reaction times. The decay of the relative abundance of the reactant ion as a function of time was used to deduce the reaction rate constants (*k*).

All the samples were obtained commercially and used as received. The nominal sample pressures were 1.2×10^{-7} to 2.5×10^{-7} Torr. The pressure readings were corrected for the sensitivity[25a] of the ion gauges and for the instrument's pressure gradient by using common procedures.[4a,23c,25b] The precision of the reaction rate measurements is better than 10%; the accuracy is estimated to be better than ±50%.

For collision-activated dissociation (CAD) experiments, the ions were cooled by allowing them to collide with a stationary pressure of argon (nominal pressure 1.2×10^{-7} Torr) for a relatively long time period (1−8 s). The isolated ions were accelerated to a preselected final kinetic energy[26] by using an on-resonance radio frequency pulse. Dissociation products for different estimated laboratory kinetic energies (12−100 eV) were measured by varying the duration of the excitation pulse. A time period of 100 ms was allowed for collisions of the accelerated ions with argon.

Standard *ab initio* molecular orbital calculations were performed using the GAUSSIAN92[27] series of programs. Optimized geometries

Scheme 2

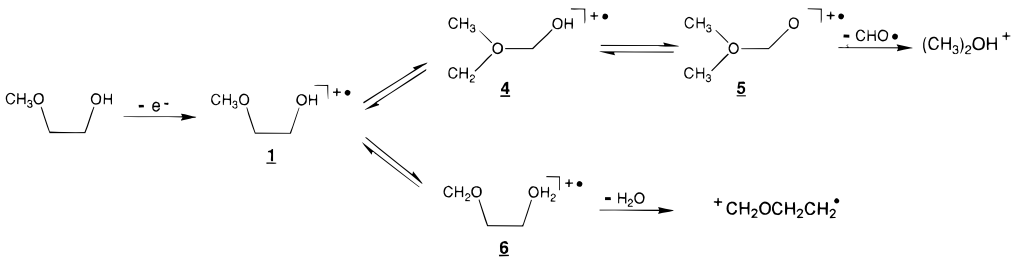

Table 1. Reaction Rate Constants, Reaction Efficiencies, and Product Ions Measured for Reactions of Ionized 2-Methoxyethanol (*m*/*z* 76, IE = 9.6 eV, PA = 182.6 kcal/mol[23a]) with Various Neutral Reagents

neutral reagent	MW	PA[a] (kcal/mol)	IE[b] (eV)	k[c]	$k_{collision}$[d]	eff[e]	primary product ions *m*/*z*	primary product ions %	reaction	secondary product ions[f] (*m*/*z*)
CH_3CHO	44	186.6	10.2	1.1	2.6	0.4	75	70	replacement of $CH_3OCH_2^{\bullet}$	89
							90	30	replacement of CH_2O	
CH_3CH_2CHO	58	189.6	10.0	1.5	2.3	0.7	89	100	replacement of $CH_3OCH_2^{\bullet}$	117
$(CD_3)_2CO$	64	196.7[g]	9.7[g]	1.9	2.3	0.8	95	100	replacement of $CH_3OCH_2^{\bullet}$	129
cyclopentanone	84	198.8	9.3	2.4	2.5	1.0	115	100	replacement of $CH_3OCH_2^{\bullet}$	169
CD_3OD	36	181.9[g]	10.9[g]	0.6	1.9	0.3	82	70	replacement of CH_2O	72−74
CH_3CH_2OH	46	188.3	10.5	1.4	1.8	0.8	77	40	replacement of $CH_3OCH_2^{\bullet}$	93
							92	60	replacement of CH_2O	
$(CH_3)_2CHOH$	60	191.2	10.1	1.4	1.8	0.8	91	60	replacement of $CH_3OCH_2^{\bullet}$	121
							106	40	replacement of CH_2O	
CH_3OCH_3	46	192.1	10.0	0.9	1.5	0.6	77	80	replacement of $CH_3OCH_2^{\bullet}$	93
							92	20	replacement of CH_2O	
CH_3CH_2I	156	≃176.0	9.3	0.8	1.6	0.5	77	20	H abstraction[h]	185[i]
							156	80	e^- transfer	(trace)
CH_3SCH_3	62	200.6	8.7	1.5	1.4	1.1	62	100	e^- transfer	none
CH_3SSCH_3	94	196.0	8.2[j]	1.8	1.9	1.0	94	100	e^- transfer	none

[a] Proton affinity values are from ref 23a. [b] Adiabatic ionization energies are from ref 23a unless otherwise noted. [c] Rate constant; $\times 10^{-9}$ cm^3 s^{-1}. [d] Collision rate ($\times 10^{-9}$ cm^3 s^{-1}) calculated according to ref 25c. [e] Efficiency = $k/k_{collision}$. [f] All the observed secondary product ions except one correspond to the proton-bound dimer of the neutral reagent. [g] Value for the corresponding undeuterated reagent. [h] H-atom abstraction by radical cations from alkyl iodides has been reported earlier; see, for example, ref 32b. [i] $CH_3CH_2I^+CH_2CH_3$. [j] Value from refs 23b and 23c.

(checked using Sybyl[28] molecular modeling software), harmonic frequencies, and zero-point vibrational energies (ZPVE) were calculated by employing spin-unrestricted Hartree−Fock (UHF) procedures carried out up to the split-valence polarization 6-31G** basis set. Single point energies were calculated for all the 6-31G** geometries by including electron correlation through the use of Møller−Plesset perturbation theory carried out to the second order (UMP2/6-31G**//UHF/6-31G**). Four different structures (**1**, **1″**, **2**, and **3**) were also optimized at the UMP2/6-31G** level. The force constant matrices calculated for all the stationary points were checked to have the correct number of negative eigenvalues (none for equilibrium structures). Since Hartree−Fock calculations are known[29] to overestimate the vibrational frequencies by 10−15%, the zero-point energies given in Table 2 were scaled by a factor of 0.9. The basis set superposition errors (BSSE) were evaluated for three structures at the UHF/6-31G** and UMP2/6-31G** levels by using the counterpoise (CP) correction procedure.[5,30a]

Results and Discussion

Structure of the Radical Cation of $CH_3OCH_2CH_2OH$. Neutral $CH_3OCH_2CH_2OH$ was ionized by electron impact or by using $CS_2^{\bullet+}$ (a more gentle method) in the dual-cell of a Fourier-transform ion cyclotron resonance (FT-ICR) mass spectrometer, transferred into the other side of the cell, isolated, collisionally cooled, and allowed to react with different neutral reagents as a function of time. The measured reaction rate constants (k), calculated collision rate constants ($k_{collision}$), and reaction efficiencies (eff = $k/k_{collision}$) are summarized in Table 1, together with the observed primary product ions, their branching ratios, and some relevant thermochemical data obtained from the literature. All the reactions were found to follow pseudo-first-order kinetics (Figure 1), suggesting that the reactant ions are likely to have a single structure and not a mixture of isomeric structures. Further support for this proposal was obtained from the finding that the product distributions and the reaction rates are independent of the method used to generate the reactant ion.

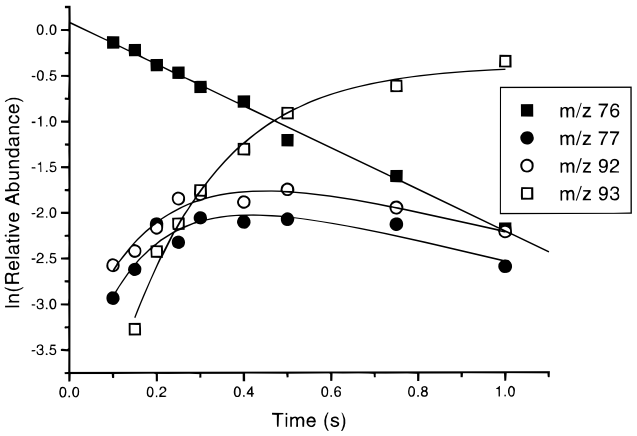

Figure 1. Temporal variation of ion abundandes upon reaction of $CH_3OCH_2CH_2OH^{\bullet+}$ with CH_3CH_2OH to yield the $CH_3OCH_2^{\bullet}$-replacement product (*m*/*z* 77) and the CH_2O-replacement product (*m*/*z* 92). Both primary product ions react with CH_3CH_2OH to yield the secondary product $(CH_3CH_2OH)_2H^+$ (*m*/*z* 93). The linear decay of the natural logarithm of the relative abundance of the reactant ion as a function of time indicates that the reaction follows pseudo-first-order kinetics.

Reaction of the radical cation with reagents with ionization energies (IE) lower than that of $CH_3OCH_2CH_2OH$ (IE = 9.6 eV[23a]) generally results in exclusive electron transfer (Table 1). For example, electron transfer dominates the reaction with CH_3SSCH_3 (IE = 8.0 eV), CH_3SCH_3 (IE = 8.7 eV), and CH_3CH_2I

(22) Burgers, P. C.; Holmes, J. L.; Terlouw, J. K.; van Baar, B. *Org. Mass Spectrom.* **1985**, *20*, 202.
(23) (a) Lias, S. G.; Bartmess, J. E.; Liebman, J. F.; Holmes, J. L.; Levin, R. D.; Mallard, W. G. *J. Phys. Chem. Ref. Data* **1988**, *17*, Supp. 1. (b) Li, W.-K.; Chiu, S.-W.; Ma, Z.-X.; Liao, C.-L.; Ng, C. Y. *J. Chem. Phys.* **1993**, *99*, 8440. (c) Leeck, D. T.; Kenttämaa, H. I. *Org. Mass Spectrom.* **1994**, *29*, 106.
(24) Wang, T.-C. L.; Ricca, T. L.; Marshall, A. G. *Anal. Chem.* **1986**, *58*, 2938.
(25) (a) Bartmess, J. E.; Georgiadis, R. M. *Vacuum* **1983**, *33*, 149. (b) Ikezoe, Y.; Matsuoka, S.; Takebe, M.; Viggiano, A. *Gas Phase Ion−Molecule Reaction Rate Constants Through 1986*; the Mass Spectroscopy Society of Japan, Tokyo, 1987. (c) Su, T.; Chesnavich, W. J. *J. Chem. Phys.* **1982**, *76*, 5183.
(26) Grosshans, P. B.; Shields, P.; Marshall, A. G. *J. Am. Chem. Soc.* **1990**, *112*, 1275.
(27) GAUSSIAN 92: Frisch, M. J.; Trucks, G. W.; Head-Gordon, M.; Gill, P. M. W.; Wong, M. W.; Foresman, J. B.; Johnson, B. G.; Schlegel, H. B.; Robb, M. A.; Replogle, E. S.; Gomperts, R.; Andres, J. L.; Raghavachari, K.; Binkley, J. S.; Gonzalez, C.; Martin, R. L.; Fox, D. J.; Defrees, D. J.; Baker, J.; Stewart, J. J. P.; Pople, J. A.; Gaussian, Inc.: Pittsburgh, PA, 1992.
(28) Tripos Associates, Inc., St. Louis, MO 63144, U.S.A.
(29) Pople, J. A.; Schlegel, H. B.; Krishnan, R.; Defrees, J. D.; Binkley, J. S.; Frisch, M. J.; Whiteside, R. A.; Hout, R. F.; Hehre, W. J. *Int. J. Quantum Chem.* **1981**, *15*, 269.
(30) (a) Boys, S. F.; Bernardi, F. *Mol. Phys.* **1970**, *19*, 553. (b) Turi, L.; Dannenberg, J. J. *J. Phys. Chem.* **1993**, *97*, 2488. (c) Turi, L.; Dannenberg, J. J. *J. Phys. Chem.* **1993**, *97*, 7899. (d) Schwenke, D. W.; Truhlar, D. G. *J. Chem. Phys.* **1985**, *82*, 2418.

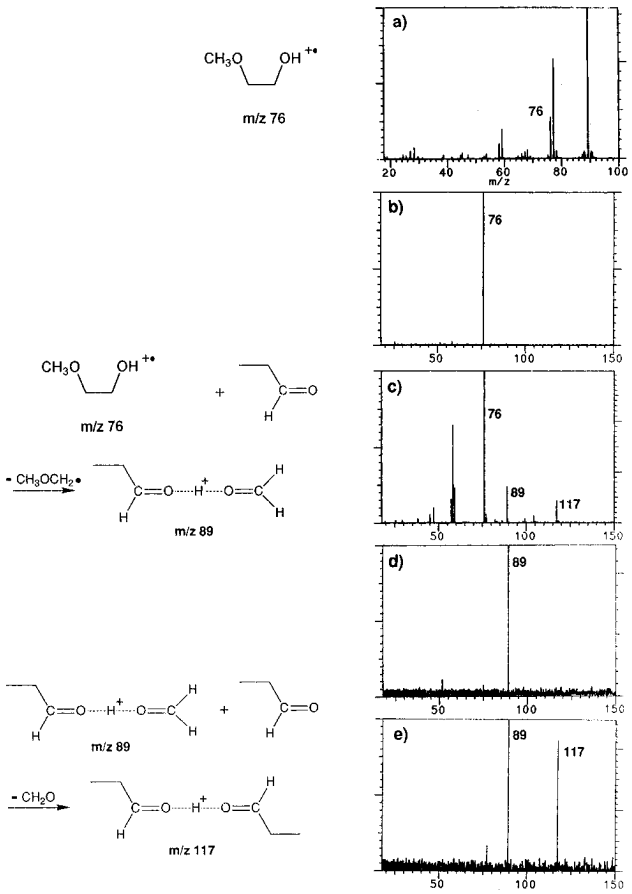

Figure 2. A typical MS/MS/MS experiment illustrated for CH_3CH_2CHO. (a) Ionization of $CH_3OCH_2CH_2OH$ by electron transfer using $CS_2^{\bullet+}$, (b) isolation of $CH_3OCH_2CH_2OH^{\bullet+}$ (*m*/*z* 76) after transfer into the other side of the dual-cell reaction chamber ($CS_2^{\bullet+}$ ions are among the isolated ions since $CS_2^{\bullet+}$ has the same nominal mass value as $CH_3OCH_2CH_2OH^{\bullet+}$), (c) reaction of $CH_3OCH_2CH_2OH^{\bullet+}$ with CH_3CH_2CHO (400 ms reaction time) to yield a major primary product ion of *m*/*z* 89 and a secondary product ion of *m*/*z* 117 (the peaks at *m*/*z* 57−59 were verified to arise from reactions of $CS_2^{\bullet+}$ with CH_3CH_2CHO by examining reactions of $CH_3OCH_2CH_2OH^{\bullet+}$ generated in the absence of CS_2), (d) isolation of the primary product ion of *m*/*z* 89, and (e) reaction of this product ion with CH_3CH_2CHO to yield the ion of *m*/*z* 117 (400 ms reaction time).

(IE = 9.3 eV). This result is expected for a radical cation with the same connectivity as in $CH_3OCH_2CH_2OH$. If the connectivities were different, the recombination energy of the ion would be likely to be significantly lower than the ionization energy of $CH_3OCH_2CH_2OH$.[31] For example, electron transfer is not commonly observed for the radical cations of molecules that after ionization isomerize to a distonic ion[13b,32] or to a hydrogen-bridged structure.[4a]

The observation of exclusive electron transfer upon reaction of the radical cation of $CH_3OCH_2CH_2OH$ with CH_3SSCH_3 is especially noteworthy. Most known distonic ions react with CH_3SSCH_3 by abstracting $CH_3S^{\bullet}$ or are unreactive.[13b,32−35] In fact, this characteristic behavior has been used to identify many distonic ions.[33−35] Hence, the absence of $CH_3S^{\bullet}$ abstraction, together with the occurrence of electron transfer, indicates that the radical cation of $CH_3OCH_2CH_2OH$ does not have a distonic structure. This finding, together with the other results discussed above, strongly suggests that the radical cation of $CH_3OCH_2CH_2OH$ has retained the connectivity of its neutral precursor.

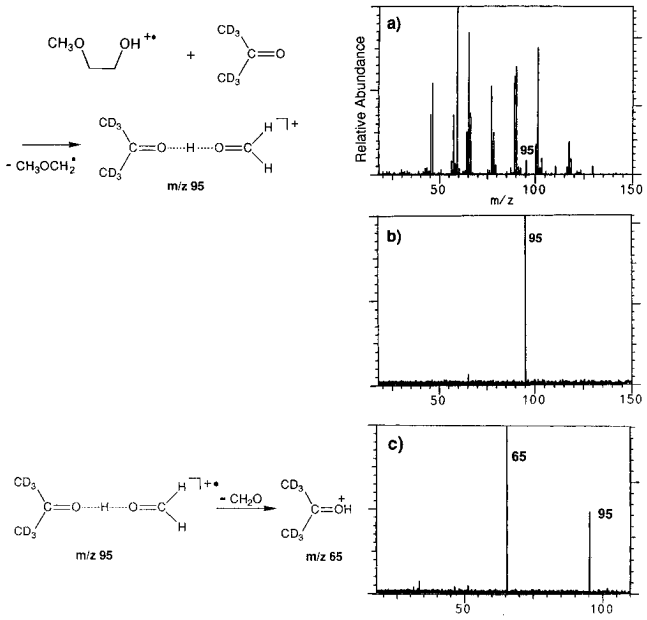

Figure 3. (a) Generation of the ion of *m*/*z* 95 by the reaction of $CH_3OCH_2CH_2OH^{\bullet+}$ with $(CD_3)_2CO$ (220 ms reaction time), (b) isolation of the ion of *m*/*z* 95 after transfer into the other side of the dual-cell reaction chamber, and (c) collision-activated dissociation of the ion of *m*/*z* 95 by using argon as the target gas at a nominal pressure of 1.2×10^{-7} Torr (100 eV estimated collision energy, 100 ms reaction time).

Replacement Reactions of $CH_3OCH_2CH_2OH^{\bullet+}$. The ion $CH_3OCH_2CH_2OH^{\bullet+}$ shows unusual reactivity toward reagents with ionization energies above that of $CH_3OCH_2CH_2OH$: facile replacement of CH_2O or $CH_3OCH_2^{\bullet}$ or both occurs (Table 1; Figures 2 and 3). These reactions are discussed below separately.

(a) $CH_3OCH_2^{\bullet}$ Replacement. The reagents CH_3CH_2OH, $(CH_3)_2CHOH$, CH_3OCH_3, CH_3CHO, CH_3CH_2CHO, $(CD_3)_2CO$, and cyclopentanone react with $CH_3OCH_2CH_2OH^{\bullet+}$ by replacement of $CH_3OCH_2^{\bullet}$ (Table 1). This reaction is probably initiated by formation of a strong hydrogen bond between the hydroxyl group of the ion and the entering neutral reagent. The energy released upon the hydrogen bond formation (approximately 30 kcal/mol[36]) likely induces the cleavage of the C−C bond in $CH_3OCH_2CH_2OH^{\bullet+}$ (Scheme 3). A precedent to this type of reactivity, cleavage of the C−C bond in $CH_3CH_2OH^{\bullet+}$ upon hydrogen bond formation, has been observed recently by others.[37] In support of the above mechanism, the reaction efficiency ($k/k_{collision}$) was found to be the highest for the neutral reagents with the greatest proton affinities (Table 1). For example, cyclopentanone (PA = 198.8 kcal/mol[23a]) replaces

(31) For example, electron abstraction by **2** ($\Delta H_f \simeq 134$ kcal/mol; assumed to be the same as ΔH_f(**1″**) as the calculations suggest; see reference 23a) would yield as the neutral products $CH_2{=}O$ (−26 kcal/mol; ref 23a), CH_3OH (−48.2 kcal/mol; ref 23a), and CH_2: (93 kcal/mol; ref 23a), or possibly $^{\bullet}CH_2OH$ (−6.2 kcal/mol; ref 23a) and $CH_3OCH_2^{\bullet}$ (−3 kcal/mol; ref 23a). Both pathways are associated with an energy release of only 5−6 eV. This is much less than is required for electron abstraction from the reagents studied here.

(32) (a) Leeck, D. T.; Stirk, K. M.; Zeller, L. C.; Kiminkinen, L. K. M.; Castro, L. M.; Vainiotalo, P.; Kenttämaa, H. I. *J. Am. Chem. Soc.* **1994**, *116*, 3028. (b) Stirk, K. M.; Smith, R. L.; Orlowski, J. C.; Kenttämaa, H. I. *Rap. Commun. Mass Spectrom.* **1993**, *7*, 392.

(33) Stirk, K. M.; Orlowski, J. C.; Leeck, D. T.; Kenttämaa, H. I. *J. Am. Chem. Soc.* **1992**, *114*, 8604.

(34) Smith, R. L.; Franklin, R. L.; Stirk, K. M.; Kenttämaa, H. I. *J. Am. Chem. Soc.* **1993**, *115*, 10348.

(35) Smith, R. L.; Kenttämaa, H. I. *J. Am. Chem. Soc.* **1995**, *117*, 1393.

(36) Formation of a hydrogen bond between two simple, gaseous, oxygen-containing molecules is typically associated with $\Delta H \approx -30$ kcal/mol; e.g., for $CH_3CH_2OH_2^+ + CH_3CH_2OH$, $\Delta H = -32$ kcal/mol; for $CH_3CH_2CH_2CH_2OH_2^+ + CH_3CH_2CH_2OH$, $\Delta H = -32$ kcal/mol; for $(CH_3CH_2)_2OH^+ + (CH_3)_2CO$, $\Delta H = -29$ kcal/mol. See: Keesee, R. G.; Castleman, A. W., Jr. *J. Phys. Chem. Ref. Data* **1986**, *15*.

(37) McMahon, T. B. Personal communication.

Scheme 3

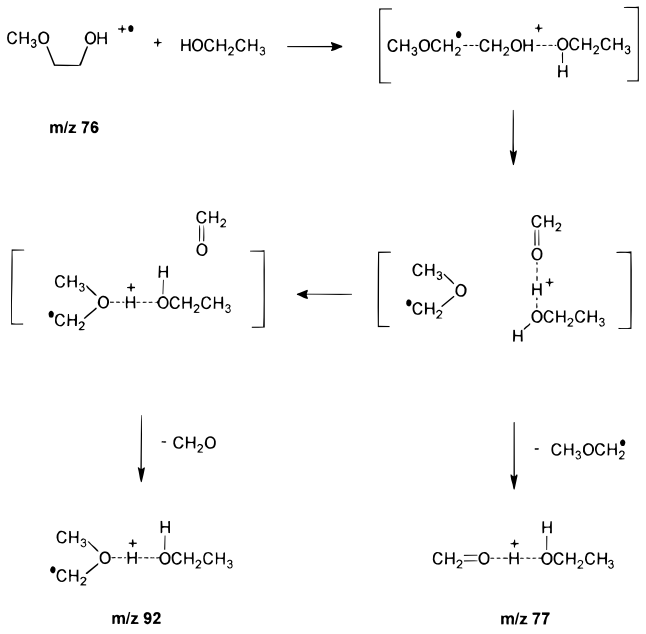

$CH_3OCH_2^\bullet$ at collision rate (efficiency 1.0). The less basic reagents $(CD_3)_2CO$ (PA = 196.7 kcal/mol) and CH_3CH_2CHO (PA = 189.6 kcal/mol) react at a lower efficiency (0.7−0.8), and CH_3CH_2OH (PA = 188.3 kcal/mol) and CH_3CHO (186.6 kcal/mol) at an even lower efficiency (0.3−0.4). The least basic reagents CD_3OD (PA = 182 kcal/mol) and CH_3CH_2I (PA = 176 kcal/mol) do not react with $CH_3OCH_2CH_2OH^{\bullet+}$ by $CH_3OCH_2^\bullet$ replacement (Table 1).

Examination of the structure of the product ions provides further support for the mechanism proposed above. According to this mechanism (Scheme 3), the $CH_3OCH_2^\bullet$-replacement product is a proton-bridged complex of the neutral reagent and CH_2O. An ion with this structure would be expected to react with nucleophiles by exclusive and facile replacement of the weaker base, CH_2O. This is exactly what was observed: *all the $CH_3OCH_2^\bullet$-replacement products undergo a facile replacement of CH_2O*, giving rise to the protonated dimer of the neutral reagent.

The reaction sequence leading to the protonated dimer of the neutral reagent was examined by multistage MS/MS/MS experiments. The experiment performed with CH_3CH_2CHO is illustrated in Figure 2. The ion $CH_3OCH_2CH_2OH^{\bullet+}$ was generated in one side of the dual cell (Figure 2a), transferred into the other cell, isolated (Figure 2b), and allowed to react with CH_3CH_2CHO (Figure 2c) to form the $CH_3OCH_2^\bullet$-replacement product expected to have the structure $CH_3CH_2CH{=}O\cdots H^+\cdots O{=}CH_2$ (*m*/*z* 89). This product ion was isolated (Figure 2d) and allowed to react with CH_3CH_2CHO (Figures 2d and 2e). Substitution of CH_2O (PA = 171.7 kcal/mol;[23a] CH_3CH_2CHO: PA = 189.6 kcal/mol[23a]) occurred to yield $CH_3CH_2CH{=}O\cdots H^+\cdots O{=}CHCH_2CH_3$ as the only observed product (*m*/*z* 117). A similar reaction sequence carried out for CH_3CHO is illustrated in Figure 4. The $CH_3OCH_2^\bullet$-replacement product $CH_3CH{=}O\cdots H^+\cdots O{=}CH_2$ (*m*/*z* 75, Figure 4a) was found to react with CH_3CHO (PA = 186.6 kcal/mol[23a]) by exclusive CH_2O replacement to yield $CH_3CH{=}O\cdots H^+\cdots O{=}CHCH_3$ as the only primary product (*m*/*z* 89, Figure 4b).

The structure of the $CH_3OCH_2^\bullet$-replacement product formed upon reaction of $CH_3OCH_2CH_2OH^{\bullet+}$ with $(CD_3)_2CO$ was also examined by collision-activated dissociation. The product ion was generated in one side of the dual-cell reaction chamber (*m*/*z* 95; Figure 3a), transferred into the other side of the cell, isolated (Figure 3b), accelerated to different laboratory kinetic energies (12−100 eV), and allowed to collide with argon. As expected[38] for the hydrogen-bridged ion $(CD_3)_2C{=}O\cdots H^+\cdots O{=}CH_2$ that is composed of two molecules with different proton affinities, the weaker base (CH_2O) is preferentially cleaved off upon excitation (CH_2O: PA = 171.7 kcal/mol;[23a] $(CD_3)_2CO$: PA = 196.7 kcal/mol[23a]). Formation of $(CD_3)_2COH^+$ dominates the reaction at all collision energies (*m*/*z* 65; Figure 3c). This result provides strong support for the proposed hydrogen-bridged structure $(CD_3)_2C{=}O\cdots H^+\cdots O{=}CH_2$ for this $CH_3OCH_2^\bullet$ replacement product.

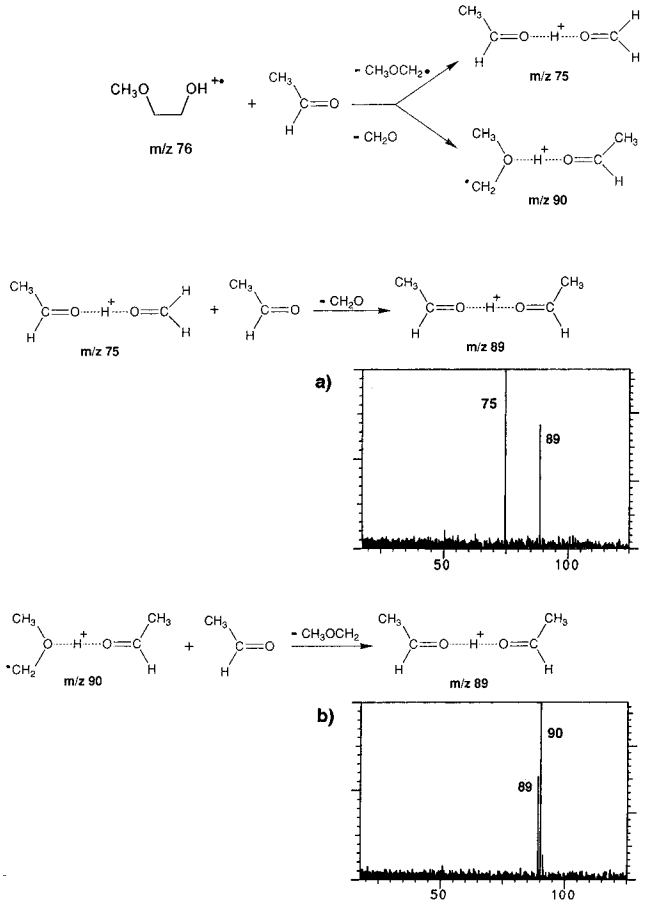

Figure 4. Spectra measured at the final stage of an MS/MS/MS experiment carried out by using CH_3CHO as the neutral reagent (nominal pressure 1.2×10^{-7} Torr): $CH_3OCH_2CH_2OH$ was ionized by electron transfer using $CS_2^{\bullet+}$, $CH_3OCH_2CH_2OH^{\bullet+}$ was isolated after transfer into the other side of the dual cell and allowed to react with CH_3CHO ($CS_2^{\bullet+}$ ions were among the isolated ions since $CS_2^{\bullet+}$ has the same nominal mass value as $CH_3OCH_2CH_2OH^{\bullet+}$; however, this does not affect the findings since $CS_2^{\bullet+}$ is unreactive toward CH_3CHO). The two product ions formed (*m*/*z* 75 and 90) were isolated. Upon reaction with CH_3CHO, both ions yield an ion of *m*/*z* 89: the ion of *m*/*z* 75 upon replacement of CH_2O (Figure 4a; 200 ms reaction time) and the ion of *m*/*z* 90 upon replacement of $CH_3OCH_2^\bullet$ (Figure 4b; reaction time 300 ms).

(b) CH_2O Replacement. Neutral reagents with proton affinities close to or less than 190 kcal/mol, i.e., CH_3OH (PA = 182 kcal/mol), CH_3CHO (PA = 186.6 kcal/mol), CH_3CH_2OH (PA = 188.3 kcal/mol), $(CH_3)_2CHOH$ (PA = 191.2 kcal/

(38) See, for example: (a) Cooks, R. G.; Patrick, J. S.; Kotiaho, T.; McLuckey, S. A. *Mass Spectrom. Rev.* In press. (b) McLuckey, S. A.; Cameron, D.; Cooks, R. G. *J. Am. Chem. Soc.* **1981**, *103*, 1313. (c) Turecek, F. In *Supplement E: The chemistry of hydroxyl, ether and peroxide groups*; Patai, E. S., Ed.; John Wiley & Sons Ltd.: Chichester, 1993; Vol. 2, pp 395−399.

Table 2. Calculated Total Energies (hartrees), Relative Energies in Parentheses (kcal/mol), Zero-Point Vibrational Energies (ZPVE, in kcal/mol), and Final Relative Energies (kcal/mol) of the $[C_3H_8O_2]^{\bullet+}$ Structures

compd	UHF/3-21G	UHF/6-31G	UHF/6-31G*	UHF/6-31G**	UMP2/6-31G**// UHF/6-31G**	ZPVE[a]	UMP2/6-31G**// UHF/6-31G**+ZPVE
$CH_3OCH_2CH_2OH^{\bullet+}$ (**1**)	−266.18356 (0)	−267.54036 (0)	−267.64794 (0)	−267.66625 (0)	−268.41105 (0)	67.77	−268.30305 (0)
$CH_3OCH_2CH_2OH^{\bullet+}$ (**1′**)	−266.17062 (8.1)	−267.52931 (6.9)	−267.63874 (5.8)	−267.65719 (5.7)	−268.39981 (7.1)	67.13	−268.29283 (6.4)
$CH_3OCH_2\cdots CH_2OH^{\bullet+}$ (**1″**)	−266.15514 (17.8)	−266.51113 (18.3)	−267.63737 (6.6)	−267.65603 (6.4)	−268.42891 (−11.2)	67.92	−268.32067 (−11.1)
$CH_3(CH_2)O-H\cdots O{=}CH_2^{\bullet+}$ (**2**)	−266.18686 (−2.1)	−267.54109 (−0.5)	−267.64543 (1.6)	−267.66491 (0.8)	−268.41952 (−5.3)	64.80	−268.31625 (−8.3)
$(CH_3)_2O-H\cdots O{=}CH^{\bullet+}$ (**3**)	−266.19700 (−8.4)	−267.54882 (−5.3)	−267.65828 (−6.5)	−267.67674 (−6.6)	−268.43756 (−16.6)	65.48	−268.33321 (−18.9)
$CH_3O(CH_2)CH_2OH^{\bullet+}$ (**4**)	−266.18262 (0.6)	−267.53047 (6.2)	−267.64073 (4.5)	−267.65961 (4.2)	−268.41809 (−4.4)	67.67	−268.31025 (−4.5)
$(CH_3)_2OCH_2O^{\bullet+}$ (**5**)	−266.19987 (−10.2)	−267.54702 (−4.2)	−267.65613 (−5.1)	−267.66922 (−1.9)	−268.41133 (0.2)	68.18	−268.30267 (0.2)
$CH_2OCH_2CH_2OH_2^{\bullet+}$ (**6**)	−266.19223 (−5.4)	−267.54449 (−2.6)	−267.64260 (3.4)	−267.66596 (0.2)	−268.42596 (−9.4)	68.20	−268.31727 (−8.9)
$CH_3OC(H)H\cdots O(H){=}CH_2^{\bullet+}$ (**7**)	−266.14807 (22.3)	−267.51759 (14.3)	−267.63415 (8.7)	−267.65340 (8.1)	−268.40414 (4.3)	65.36	−268.29998 (1.9)

[a] Calculated at the UHF/6-31G** level of theory and scaled by a factor of 0.9.

mol), and CH_3OCH_3 (PA = 192.1 kcal/mol), replace CH_2O in $CH_3OCH_2CH_2OH^{\bullet+}$. This reaction is likely initiated by $CH_3OCH_2^{\bullet}$ replacement within the collision complex, as discussed above. If the $CH_3OCH_2^{\bullet}$ replacement is highly exothermic, the resulting complex dissociates rapidly to $CH_3OCH_2^{\bullet}$ and the hydrogen-bridged complex of CH_2O and the neutral reagent (i.e., $CH_3OCH_2^{\bullet}$ replacement occurs; some of these reactions were found to be so exothermic that the ion produced is metastable and slowly dissociates by the loss of CH_2O). However, reactions of less basic reagents will yield a lower-energy and longer-lived ion−molecule complex. Within this complex, $CH_3OCH_2^{\bullet}$ can react with the $CH_3OCH_2^{\bullet}$-replacement product (Scheme 3) to replace CH_2O (the weaker base: PA = 172 kcal/mol for CH_2O; PA = 173 kcal/mol[39] for $CH_3OCH_2^{\bullet}$).

According to the mechanism proposed above, the final ionic product is a hydrogen-bridged complex of $^{\bullet}CH_2OCH_3$ and the neutral reagent molecule. Examination of the reactivity of the product ion (*m*/*z* 90) formed upon the reaction of CH_3CHO suggests that this ion indeed has the expected structure $^{\bullet}CH_2O(CH_3)\cdots H^+\cdots O{=}CHCH_3$: this ion reacts with CH_3CHO (PA = 186.6 kcal/mol[23a]) by a facile replacement of $CH_3OCH_2^{\bullet}$ (PA = 173 kcal/mol[39]) to generate $CH_3CH{=}O\cdots H^+\cdots O{=}CHCH_3$ (*m*/*z* 89, Figure 4c, 4f, and 4g).

It is noteworthy that the reactions of $CH_3OCH_2CH_2OH^{\bullet+}$ lead to the formation of stable hydrogen-bridged complexes of the neutral reagent and $CH_3OCH_2^{\bullet}$. The ion $CH_3OCH_2CH_2OH^{\bullet+}$ provides a tool for the strategic synthesis of a variety of hydrogen-bridged complexes of the type $^{\bullet}CH_2O(CH_3)\cdots H^+\cdots N$ wherein N is the neutral reagent used.

Molecular Orbital Calculations. *Ab initio* molecular orbital calculations using the GAUSSIAN92[27] program were performed to study the relative stabilities of seven isomeric $C_3H_8O_2^{\bullet+}$ structures. Several possible conformers were examined for each isomer. Only the most stable conformers are discussed here (see Tables 2−5), with the exception of the ion $CH_3OCH_2CH_2OH^{\bullet+}$. For this ion, results obtained for three different conformations are presented (**1**, **1′**, and **1″**). All the structures were optimized in a stepwise manner up to the UHF/6-31G** level of theory. The structures **1**, **1″**, **2**, and **3** were also optimized at the UMP2/6-31G** level (Figure 5; Tables 4 and 5). The lowest energy structures obtained at this level of theory differ in some respects from those obtained at the UHF level (UHF/6-31G**). For example, the long bond lengths in the UHF/6-31G** optimized structures **1″** (C_2-C_3), **2** (O_2-H_6), and **3** (O_2-H_7) are shorter at the electron correlation level (Figure 5). These results are discussed in detail below. The extent of spin contamination, as indicated by $\langle S^2\rangle$, was found to be within an acceptable range (0.756−0.767) and close to the value of 0.75 for the pure spin state in all the calculations.

Basis set superposition errors (BSSE) were evaluated for the ions **1″**, **2**, and **3** by using the counterpoise method, expected to provide an upper limit for BSSE.[30] For an ion A···B, this method involves calculating the sum (*e*(sum); see Tables 3 and 5) of the energy differences (*e*(A) and *e*(B)) between the energies

Table 3. Counterpoise Corrections for the Basis Set Superposition Errors (BSSE), *e*, Calculated with the UHF/6-31G** Basis Set (values in kcal/mol)

structure	*e*(A)[a]	*e*(B)[b]	*e*(sum)
$CH_3OCH_2\cdots CH_2OH^{\bullet+}$ (**1″**)	*e*($CH_3OCH_2^+$) 0.62	*e*($^{\bullet}CH_2OH$) 1.72	2.34
$CH_3(CH_2)O-H\cdots O{=}CH_2^{\bullet+}$ (**2**)	*e*($CH_3(^{\bullet}CH_2)O^+H$) 0.16	*e*(CH_2O) 0.87	1.03
$(CH_3)_2O-H\cdots O{=}CH^{\bullet+}$ (**3**)	*e*($(CH_3)_2O^+H$) 0.14	*e*($^{\bullet}CHO$) 0.65	0.79

[a] e(A) is the correction obtained for the fragment A in the presence of the atomic orbitals of the B fragment. [b] *e*(B) is the correction obtained for the fragment B in the presence of the atomic orbitals of the A fragment.

Table 4. The Energies (hartrees), Relative Energies in Parentheses (kcal/mol), Zero-Point Vibrational Energies (ZPVE, in kcal/mol), and Final Relative Energies (kcal/mol) of Four-Structures Calculated at the Electron Correlation Level

compd	UMP2/ 6-31G**	ZPVE[a]	UMP2/ 6-31G**+ZPVE
$CH_3OCH_2CH_2OH^{\bullet+}$ (**1**)	−268.41491 (0)	64.21	−268.31257 (0)
$CH_3OCH_2\cdots CH_2OH^{\bullet+}$ (**1″**)	−268.43540 (−12.9)	66.73	−268.32906 (−10.4)
$CH_3(CH_2)O-H\cdots O{=}CH_2^{\bullet+}$ (**2**)	−268.42395 (−5.7)	62.04	−268.32508 (−7.9)
$(CH_3)_2O-H\cdots O{=}CH^{\bullet+}$ (**3**)	−268.44110 (−16.4)	63.07	−268.34059 (−17.6)

[a] Calculated at the UMP2/6-31G** level of theory and scaled by a factor of 0.9.

(39) Estimated from the heat of formation of $CH_3OCH_2^{\bullet}$ = −3 kcal/mol (ref 23a) and from a calculated heat of formation of $CH_3O(H^+)CH_2^{\bullet}$ = 190 kcal/mol; see: (a) Bouma, W. J.; Nobes, R. H.; Radom, L. *Org. Mass Spectrom.* **1982**, *17*, 315. (b) Bouma, W. J.; Nobes, R. H.; Radom, L. *J. Am. Chem. Soc.* **1983**, *105*, 1746.

Table 5. Counterpoise Corrections for the Basis Set Superposition Errors (BSSE), *e*, Calculated with the UMP2/6-31G** Basis Set (in kcal/mol)

structure	*e*(A)[a]	*e*(B)[b]	*e*(sum)
$CH_3OCH_2\cdots CH_2OH^{\bullet+}$ (**1″**)	*e*($CH_3OCH_2^{\bullet}$)	*e*(CH_2OH^+)	
	3.63	2.00	5.63
$CH_3(CH_2)O-H\cdots O{=}CH_2^{\bullet+}$ (**2**)	*e*($CH_3(^{\bullet}CH_2)O^+H$)	*e*(CH_2O)	
	0.62	2.64	3.26
$(CH_3)_2O-H\cdots O{=}CH^{\bullet+}$ (**3**)	*e*($(CH_3)_2O^+H$)	*e*($^{\bullet}CHO$)	
	0.44	1.64	2.08

[a] *e*(A) is the correction obtained for the fragment A in the presence of the atomic orbitals of the B fragment. [b] *e*(B) is the correction obtained for the fragment B in the presence of the atomic orbitals of the A fragment.

of the isolated fragments (*E*(A) and *E*(B)) and the energy of the corresponding fragment with the basis set of the whole ion (e.g., for A, this involved calculation of E_{AB}(A) by including the ghost orbitals of B; *e*(sum) = *e*(A) + *e*(B) = [*E*(A) − E_{AB}(A)] + [*E*(B) − E_{AB}(B)]).[5,30] The counterpoise estimates were found to be relatively small (1−2 kcal/mol) at the UHF level but greater (2−6 kcal/mol) at the UMP2 level, as expected.[5,30] The orbital space of the fragments $^{\bullet}CH_2OH$, CH_2O, and $^{\bullet}CHO$ is more affected by the ghost orbitals than that of $CH_3OCH_2^+$, $CH_3(CH_2)OH^{\bullet+}$, and $(CH_3)_2OH^+$. Overall, the counterpoise estimates suggest that BSSE has only a small effect on the relative energies of the ions **1″**, **2**, and **3**. At the UMP2/6-31G**+ZPVE level of theory, the relative energies of **1″**, **2**, and **3** were found to change from 0, 2.5, and −7.2 kcal/mol to 0, 0.1, and −10.8 kcal/mol, respectively.

The energies of **1′** and **2** (relative to that of **1**) were found to be fairly independent of the level of theory employed. The relative stability of the structure **5** decreases with the increasing size of the basis set but eventually converges to that of **1**. The opposite is true for the remaining structures (**1″**, **3**, **4**, **6**, and **7**). The relative energies of the structures **1″**, **3**, **4**, and **6** decrease most dramatically when electron correlation was included, *e.g.*, for **3**, UHF/6-31G** yields −6.6 kcal/mol *vs* UMP2/6-31G**//UHF/6-31G** yields −16.6 kcal/mol and UMP2/6-31G** yields −16.4 kcal/mol. The relative energies calculated at the UMP2/6-31G**+ZPVE level for the structures optimized at UHF/6-31G** and UMP2/6-31G** levels were found to be nearly equal.

The relative energies of a large number of conformations of $CH_3OCH_2CH_2OH$ have been calculated earlier.[18] The calculations of the covalently bonded $CH_3OCH_2CH_2OH^{\bullet+}$ included the most stable of these conformations as the initial input structures, such as the hydrogen-bridged structure shown in Scheme 1. All these conformers were allowed to optimize freely (no geometry constraints were employed). None of the final optimized structures contained stabilizing intramolecular hydrogen bonding. For example, optimization of the hydrogen-bridged structure shown in Scheme 1 yielded **1** as the optimized structure (Figure 5).

The ion $CH_3OCH_2CH_2OH^{\bullet+}$ with the linear geometry **1′** lies 6.4 and 17.5 kcal/mol higher in energy, respectively, than the two bent structures **1** and **1″** (UMP2/6-31G**//UHF/6-31G**+ZPVE level of theory; Table 2; Figure 5). The most stable structure **1″** is characterized by a remarkably long C−C bond (1.969 Å *vs* 1.521 Å (**1**) and 1.518 Å (**1′**); UHF/6-31G**). The structure **1″** also contains an unusually short CH_3O-CH_2 bond (1.285 Å *vs* 1.466 Å (**1**) and 1.464 Å (**1′**)) and a slightly shorter $HO-CH_2$ bond than the other two structures (1.308 Å *vs* 1.391 Å (**1**) and 1.386 Å (**1′**)). Hence, the structure **1″** is best described as a loosely bonded complex of $CH_3OCH_2^{\bullet}$ and CH_2OH^+. At the UMP2/6-31G** level of theory (Figure 5), the minimum energy geometry of **1″** is similar to that obtained

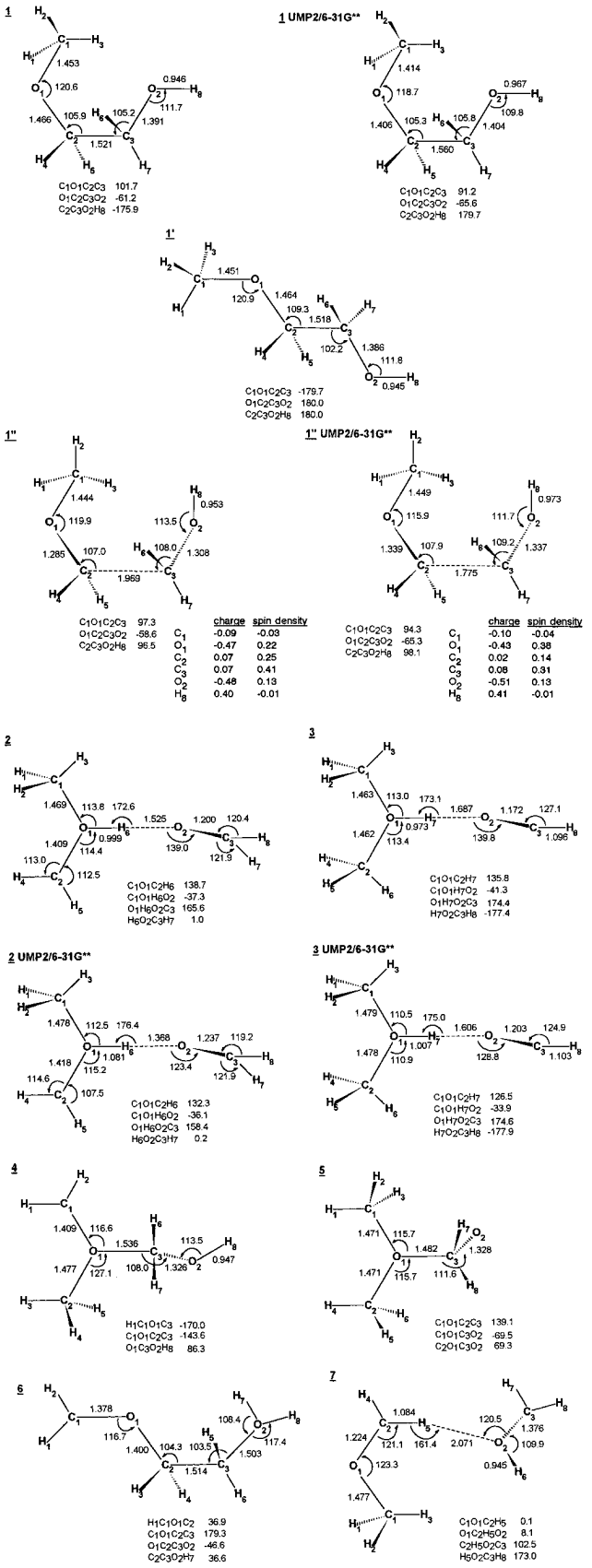

Figure 5. UHF/6-31G** and UMP2/6-31G** (marked as such) optimized geometries for different $[C_3H_8O_2]^{\bullet+}$ isomers.

at the UHF/6-31G** level. However, the C−C bond in the UMP2/6-31G** optimized structure is slightly shorter (1.775 Å). The presence of a long C−C bond in an organic radical cation is not unprecedented: the ions $CH_3CH_2OH^{\bullet+}$ and $HOCH_2-CH_2OH^{\bullet+}$ have been calculated to have structures with remark-

ably long one-electron C−C bonds ($CH_3CH_2OH^{\bullet+}$, 2.013 Å at the UHF/4-31G level;[40a,b] $HOCH_2CH_2OH^{\bullet+}$, 2.01 Å at the RHF/DZP level[40c]). The results obtained in the above calculations, especially the long C−C bond in **1″**, as well as the location of the greatest positive charge at the hydroxyl hydrogen in this ion (Figure 5), support the proposal that the entering nucleophile initially forms a hydrogen bond with the hydroxyl hydrogen, as shown in Scheme 3.

As pointed out above, the internally excited ion $CH_3OCH_2CH_2OH^{\bullet+}$ has been suggested to equilibrate with the distonic ions $^{\bullet}CH_2O^+(CH_3)CH_2OH$ (**4**), $(CH_3)_2O^+CH_2O^{\bullet}$ (**5**), and $^{\bullet}CH_2OCH_2CH_2OH_2^+$ (**6**) prior to or during dissociation (Scheme 2).[20] The most stable geometries found for these distonic ions lie 6.9, 11.3, and 2.2 kcal/mol higher in energy than **1″**, respectively (at the UMP2/6-31G**//UHF/6-31G**+ZPVE level of theory). Hence, it is not surprising that these distonic ions are not generated from the nondissociating ion $CH_3OCH_2CH_2OH^{\bullet+}$ in the experiments discussed above. The ion $^{\bullet}CH_2OCH_2CH_2OH_2^+$ (**6**) is more stable by 5.6 kcal/mol and 9.0 kcal/mol, respectively, than the distonic ions $^{\bullet}CH_2O^+(CH_3)CH_2OH$ (**4**) and $(CH_3)_2O^+CH_2O^{\bullet}$ (**5**) (at the UMP2/6-31G**//UHF/6-31G**+ZPVE level of theory). The most stable geometry of the ion **6** is stabilized by an intramolecular hydrogen bond (1.908 Å) between the C−O−C oxygen and one of the C−O−H hydrogens (note the small $O-CH_2-CH_2$, $CH_2-CH_2-OH_2$, and CH_2-O-H bond angles: 104.3°, 103.5°, and 108.4°, respectively). The length of the CH_2O-CH_2 bond (1.378 Å) indicates that the bond has considerable double bond character.

The most stable geometry of the ion $^{\bullet}CH_2O(CH_3)-H^+\cdots O{=}CH_2$ (**2**) was found to be slightly less stable than **1″** (by 2.5 kcal/mol at the UMP2/6-31G**+ZPVE level of theory). In contrast, the ion $(CH_3)_2O-H^+\cdots O{=}CH^{\bullet}$ (**3**) is more stable than **1″** by 7.2 kcal/mol (at the UMP2/6-31G**+ZPVE level of theory). Experimental evidence does not support the formation of either one of these ions upon ionization of $CH_3OCH_2CH_2OH$. Exclusive replacement of CH_2O is expected for an ion with structure **2** since CH_2O is bonded less strongly than $CH_3OCH_2^{\bullet}$ in the ion (the $-O\cdots H\cdots O$ bond length to $CH_3OCH_2^{\bullet}$ is 0.999 Å while that to CH_2O is 1.525 Å). In the ion **3**, $HCO^{\bullet}$ is the less strongly bonded fragment (the hydrogen bond to CH_3OCH_3 is 0.973 Å while that to $HCO^{\bullet}$ is 1.687 Å). Hence, this ion would be identified by a facile replacement of $HCO^{\bullet}$, a reaction that was not observed in any of the experiments.

Finally, the complex $CH_3OC(H)H\cdots O(H){=}CH_2^{\bullet+}$ (**7**) was also examined computationally. In the most stable geometry examined, CH_2OH^+ and $CH_3OCH_2^{\bullet}$ are connected chiefly by weak electrostatic forces, as indicated their great separation (2.071 Å). This ion was found to lie significantly higher in energy (13 kcal/mol) than the ion **1″**.

(40) (a) Bouma, W. J.; Dawes, J. M.; Radom, L. *Org. Mass Spectrom.* **1983**, *18*, 12. (b) Postma, R.; Ruttink, P. J. A.; Van Baar, B.; Terlouw, J. K.; Holmes, J. L.; Burgers, P. C. *Chem. Phys. Lett.* **1986**, *123*, 409. (c) Ruttink, P. J. A.; Burgers, P. C. *Org. Mass Spectrom.* **1993**, *28*, 1087.

Conclusions

Examination of the gas-phase reactions of the long-lived, low-energy radical cation generated from $CH_3OCH_2CH_2OH$ suggests that the connectivity of $CH_3OCH_2CH_2OH$ does not change upon ionization. The ion $CH_3OCH_2CH_2OH^{\bullet+}$ undergoes gas-phase reactions quite unique for an organic radical cation: neutral reagents replace $CH_3OCH_2^{\bullet}$ in the ion. The reaction is likely initiated by the formation of a strong hydrogen bond between the entering nucleophile and the hydroxyl group in $CH_3OCH_2CH_2OH^{\bullet+}$. The exothermicity of the hydrogen bond formation (about 30 kcal/mol) drives the cleavage of the C−C bond. A precedent to this type of reactivity has been proposed earlier for $CH_3CH_2OH^{\bullet+}$.[37] Dissociation of the internally excited ions $CH_3OCH_2CH_2OH^{\bullet+}$ by the loss of $CHO^{\bullet}$ (Scheme 2) is also thought to be initiated by the cleavage of the C−C bond.[20] All these findings are in agreement with the finding of a remarkably long C−C bond in the most stable structure calculated for $CH_3OCH_2CH_2OH^{\bullet+}$ (UMP2/6-31G**).

Weak nucleophiles react with $CH_3OCH_2CH_2OH^{\bullet+}$ through an additional channel. Replacement of $CH_3OCH_2^{\bullet}$ with weak nucleophiles yields a long-lived ion−molecule complex that can undergo further reactions. Within this complex, $CH_3OCH_2^{\bullet}$ replaces CH_2O (a weaker base) to form the hydrogen-bridged complex of $CH_3OCH_2^{\bullet}$ and the neutral reagent. This reaction provides a general synthetic route to stable hydrogen-bridged radical cations in the gas phase.

Ab initio molecular orbital calculations (UMP2/6-31G**//UHF/6-31G**+ZVPE) suggest that the ion $CH_3OCH_2CH_2OH^{\bullet+}$ lies 6.6, 11.3, and 2.2 kcal/mol lower in energy than the distonic ions $^{\bullet}CH_2O^+(CH_3)CH_2OH$ (**4**), $(CH_3)_2O^+CH_2O^{\bullet}$ (**5**), and $^{\bullet}CH_2OCH_2CH_2OH_2^+$ (**6**), respectively. Hence, although the internally excited radical cation $CH_3OCH_2CH_2OH^{\bullet+}$ may equilibrate with these distonic ions prior to or during dissociation (Scheme 2),[20] it is not surprising that the long-lived, low-energy ions do not undergo equilibration.

Acknowledgment. The Academy of Finland, University of Joensuu, and the Finnish Chemical Society, as well as the National Science Foundation (CHE-9409644), are thanked for partial financial support of this work. Chris L. Stumpf is thanked for running some of the experiments.

JA952145P